

Coupling Between a Viscoelastic Gas/Liquid Interface and a Swirling Vortex Flow

J. M. Lopez

Associate Professor,
Department of Mathematics,
Arizona State University,
Tempe, AZ 85287

J. Chen

Staff Scientist,
COMSAT Laboratories,
22300 COMSAT Drive,
Clarksburg, MD 20871

While the structure and dynamics of boundary layers on rigid no-slip walls in rotation dominated enclosed flows are still an area of active research, the interactions between rotating or swirling flows with a free surface have received comparatively less attention. For the most part, investigations in this area have been focused on clean free surfaces, which may be treated as stress-free. However, in most practical situations the surface is rarely clean, and even under laboratory conditions, it is quite difficult to achieve a clean free surface. Most impurities in liquids are surface active, and hence the name surface active agent or surfactant. These surfactants tend to establish an equilibrium surface concentration which alters the interfacial tension and interfacial viscoelastic properties of the gas/liquid interface. The coupling between the bulk swirling flow and the interface is provided via the tangential stress balances, and these stresses on the interface are dependent upon the surface concentration of surfactant, which in turn is altered by the interfacial flow. Forces acting on the interface include surface tension gradients (elastic) and the viscous resistance to shear and dilatation. These viscoelastic properties vary with the surfactant concentration on the surface. Here, we present numerical studies of flow in a cylinder driven by the constant rotation of the bottom endwall with the top free surface being contaminated by a Newtonian surfactant. Comparisons with a clean free surface and a no-slip stationary top endwall provide added insight into the altered dynamics that result from the presence of a small amount of surfactant.

1 Introduction

Many geophysical and industrial flows are dominated by gas/liquid interfaces. Gas/liquid interfaces in general, and the ocean surface in particular, are rarely free of surfactants. The amount of surfactant required to have a significant effect on the hydrodynamic behavior of the interface can be as low as a fraction of a kg km^{-2} , and the surface tension may be halved with 1 kg km^{-2} of many surfactants. At these concentrations, surfactants form an expanded monomolecular surface film or monolayer. Surfactants make the interface not only elastic (surface tension variations as a result of variations in the surfactant surface concentration), but also give it surface (or excess) viscosity, which can be many orders of magnitude larger than the viscosity in the bulk multiplied by an appropriate bulk flow length scale (Hirsa et al., 1997a). In many fluid dynamic systems which have a gas/liquid interface (even when the ratio of inertial to surface tension forces is large), the transport of mass, momentum, and energy is strongly influenced by the viscoelastic nature of the interface; for high Reynolds number flows see Hunt (1984), Asher and Pankow (1991), Hirsa et al. (1995), and for low Reynolds number flows see Grotberg (1994).

In recent years it has been demonstrated that at any instant, the bulk flow near an air/water interface with surfactant is described by interfacial boundary conditions ranging from a clean free surface to a state with characteristics similar to that of a solid wall (Tryggvason et al., 1992; Tsai and Yue, 1995). The variations in the interfacial boundary conditions are dependent on the concentration levels and viscoelastic properties of the surfactant. Furthermore, not only does the presence of a surfactant alter the subsurface flow, but also the subsurface flow alters the conditions on the surface, primarily by redistributing

the surfactant on the interface and to/from the bulk. This leads to a coupled nonlinear system rich in dynamical behavior.

We address not only the influence that the interfacial stress imparts upon the hydrodynamics in the bulk, but also the influence of the bulk flow on the dynamics of the interface. When the interface is covered by surfactants, a boundary layer (comparable to the boundary layer on a solid wall) can form at the interface with both elastic and viscous properties. The formation of the free surface boundary layer significantly increases wave damping; it also alters gas transfer rates, reduces turbulence by shedding surface parallel vortices, and tilts surface-normal vorticity, among other effects. It is essential to understand this dynamic nonlinear coupling between the interior flow and the surface processes in order to be able to interpret observations of surface flows and to develop predictive capabilities for both the surface and the subsurface flows.

Studies incorporating the hydrodynamic coupling with the interface have typically included the elastic effects due to surface tension variations (e.g., Foda and Cox 1980; Wang and Leighton 1990; Tryggvason et al., 1992; Ananthakrishnan and Yeung, 1994; Grotberg, 1994). These studies considered the interface itself as being inviscid. The experiments of Hirsa et al. (1995) showed that in flows where the surface velocity field is solenoidal, the surface shear viscosity has a significant influence on the subsurface velocity field. The surface shear viscosity is a relatively easy property to measure, however experiments (Maru and Wasan, 1979) have shown that the surface dilatational viscosity may be several orders of magnitude larger and is a difficult property to quantify (Edwards et al., 1991). The recent study by Tsai and Yue (1995) included for the first time both surface viscosities in hydrodynamic computations of the interactions of surface-parallel vorticity with a contaminated air/water interface in planar two-dimensional flows. However, they treated these as constant coefficients whereas it is known (Maru and Wasan, 1979; Tsai and Yue, 1995) that these quantities vary with, amongst other things, the surface concentration

Contributed by the Fluids Engineering Division for publication in the JOURNAL OF FLUIDS ENGINEERING. Manuscript received by the Fluids Engineering Division November 5, 1997; revised manuscript received July 13, 1998. Guest Editor: D. T. Valentine.

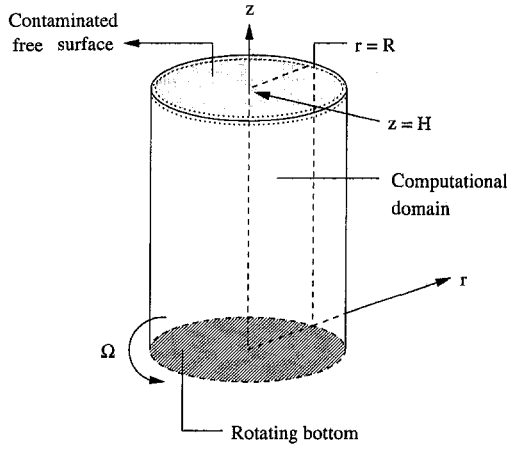


Fig. 1 Schematic of the model flow

of the surfactant. Further, in the flows they considered the surface velocity is everywhere normal to the surface vorticity and both are tangent to the surface. Here, we consider flows where the inner product of surface velocity and surface vorticity is not identically zero, and also the surface viscosities are functions of surface concentration. We derive the appropriate interfacial conditions by balancing the tangential stresses at the interface, written in terms of the surface vorticity, and couple these to a Navier-Stokes solver for the whole flow. The formulation is applied to a model problem that is chosen to isolate and highlight individual processes. The model problem is that of flow in an open cylinder driven by the constant rotation of the bottom endwall with the top free surface covered by a monolayer of insoluble surfactant. A schematic is given in Fig. 1.

It is often seen that the elastic effects, due to surface tension gradients, lead to flow instability (Sternling and Scriven, 1959), and that interfacial viscosity effects tend to damp these instabilities. This is generally true when the vorticity in the bulk flow is predominantly surface-parallel. However, when the vorticity near the interface is predominantly surface-normal, the interfacial viscous effects dominate the dynamics. The interfacial viscous effects provide a mechanism for the tilting of surface-normal vorticity, in an analogous manner that molecular viscosity does at a rigid wall, and leads to secondary motions, boundary layer formation, boundary layer separation, internal shear layers, etc. Once the surface-normal vorticity is tilted into surface-parallel vorticity, the elastic effects at the interface also come into play, and there is a dynamic interaction between the elasticity and the viscosity on the surface and the vortical flow in the bulk.

2 Interfacial Rheology and the Development of Boundary Conditions for Vorticity at a Contaminated Interface

We shall be concerned here with non-deforming surfaces, i.e., negligible Froude number flow. The physical flows that this formulation is primarily being derived for involve very little free surface deformation regardless of the amount of surfactant (Spohn et al., 1993). Also, we consider here axisymmetric flow as it contains the hydrodynamics of interest (both surface-normal and surface-parallel vorticity, and the turning and stretching of vorticity).

The governing equations are the axisymmetric Navier-Stokes equations, together with the continuity equation and appropriate boundary and initial conditions. Using a cylindrical polar coordinate system (r, θ, z) and the Stokes streamfunction ψ , the nondimensional velocity vector is $\mathbf{u} = (u, v, w) = (-1/r \partial \psi / \partial z, \Gamma/r, 1/r \partial \psi / \partial r)$ and the associated vorticity vector is $\boldsymbol{\omega} =$

$(-1/r \partial \Gamma / \partial z, \eta, 1/r \partial \Gamma / \partial r)$. The nondimensional axisymmetric Navier-Stokes equations are:

$$\frac{D\Gamma}{Dt} = \frac{1}{\text{Re}} \nabla_*^2 \Gamma, \quad (2.1)$$

$$\frac{D\eta}{Dt} + \frac{\eta}{r^2} \frac{\partial \psi}{\partial z} - \frac{1}{r^3} \frac{\partial \Gamma^2}{\partial z} = \frac{1}{\text{Re}} \left(\nabla^2 \eta - \frac{\eta}{r^2} \right), \quad (2.2)$$

where

$$\nabla_*^2 \psi = -r\eta,$$

$$\text{Re} = \Omega R^2 / \nu,$$

$$\frac{D}{Dt} = \frac{\partial}{\partial t} - \frac{1}{r} \frac{\partial \psi}{\partial z} \frac{\partial}{\partial r} + \frac{1}{r} \frac{\partial \psi}{\partial r} \frac{\partial}{\partial z},$$

$$\nabla^2 = \frac{\partial^2}{\partial z^2} + \frac{\partial^2}{\partial r^2} + \frac{1}{r} \frac{\partial}{\partial r},$$

$$\nabla_*^2 = \frac{\partial^2}{\partial z^2} + \frac{\partial^2}{\partial r^2} - \frac{1}{r} \frac{\partial}{\partial r},$$

ν is the kinematic viscosity, $1/\Omega$ is the time scale and R is the length scale, where $\Omega \text{ rad s}^{-1}$ is the rate of rotation of the bottom endwall and R is the radius of the cylinder, which is filled to a depth H .

We begin our treatment of the interface by considering the Boussinesq-Scriven surface fluid model (Boussinesq, 1913; Scriven, 1960; Slattery, 1990):

$$\mathbf{T}^s = (\sigma^* + (\kappa^s - \mu^s) \text{div}_s \cdot \hat{\mathbf{u}}^s) \mathbf{I}_s + 2\mu^s \mathbf{D}^s, \quad (2.3)$$

where the surface stress tensor \mathbf{T}^s is described as a linear function of the surface rate of deformation tensor

$$2\mathbf{D}^s = (\nabla_s \hat{\mathbf{u}}^s \cdot \mathbf{I}_s + \mathbf{I}_s \cdot (\nabla_s \hat{\mathbf{u}}^s)^T).$$

In this constitutive equation, κ^s is the surface dilatational viscosity, μ^s is the surface shear viscosity, σ^* is the thermodynamic interfacial tension, $\hat{\mathbf{u}}^s$ is the surface velocity, div_s is the surface divergence operator, ∇_s is the surface gradient operator, and \mathbf{I}_s is the tensor that projects any vector onto the interface. The surface stress $\boldsymbol{\tau}$ can then be expressed as (Slattery 1990):

$$\boldsymbol{\tau} = \nabla_s \sigma^* + \nabla_s \cdot ((\kappa^s - \mu^s) \text{div}_s \hat{\mathbf{u}}^s) + 2(\nabla_s \mu^s) \cdot \mathbf{D}^s + 2\mu^s \text{div}_s \mathbf{D}^s.$$

Noting that there is no slip at the interface, so the tangential component of fluid velocity is continuous across the interface, we balance the above surface stresses with the corresponding components from the bulk flow, using cylindrical polars and nondimensionalizing σ^* with σ_i , a characteristic value of the surface tension, so that $\sigma = \sigma^* / \sigma_i$, and putting $\lambda_\mu = \mu^s / \mu R$, $\lambda_\kappa = \kappa^s / \mu R$, and $\lambda_{\kappa+\mu} = \lambda_\kappa + \lambda_\mu$, where μ is the shear viscosity of the bulk fluid, the nondimensional stress balance in the azimuthal direction is

$$\frac{\partial \Gamma}{\partial z} = \lambda_\mu \left(\frac{\partial^2 \Gamma}{\partial r^2} - \frac{1}{r} \frac{\partial \Gamma}{\partial r} \right) + \frac{\partial \lambda_\mu}{\partial r} \left(\frac{\partial \Gamma}{\partial r} - \frac{2\Gamma}{r} \right), \quad (2.4)$$

and in the radial direction

$$\eta = C_a \frac{\partial \sigma}{\partial r} + \lambda_{\kappa+\mu} \left(\frac{1}{r^2} \frac{\partial^2 \psi}{\partial r \partial z} - \frac{1}{r} \frac{\partial^3 \psi}{\partial r^2 \partial z} \right) - \frac{1}{r} \frac{\partial^2 \psi}{\partial r \partial z} \frac{\partial \lambda_{\kappa+\mu}}{\partial r} + \frac{2}{r^2} \frac{\partial \psi}{\partial z} \frac{\partial \lambda_\mu}{\partial r}, \quad (2.5)$$

where $C_a = \sigma_i / \mu \Omega R$ is the capillary number.

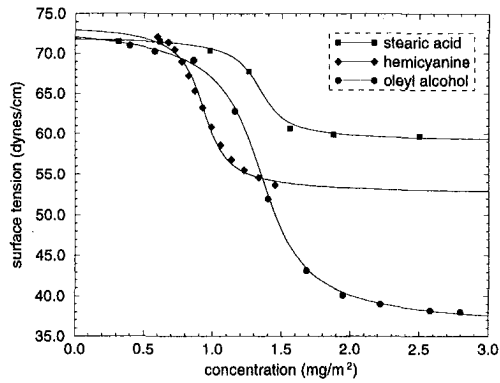


Fig. 2 Nonlinear equations of state for various surfactant/water systems; symbols are experimental measurements of Kim (1996) and solid lines correspond to model Eq. (2.6)

Equations (2.4) and (2.5) represent the balance of forces on a surface element resulting from viscous traction or shearing stress from the bulk, surface tension (or surface pressure) gradients, and surface viscosity effects. Their solution for Γ and η on the interface provide the boundary conditions for the bulk flow Eqs. (2.1) and (2.2). Note that Eqs. (2.4) and (2.5) are also coupled to the bulk flow through normal derivative terms in Γ and ψ , respectively, at the interface. It is clear that the stress balance in the azimuthal direction does not include any elastic term, only surface shear viscosity terms. If the flow near the interface is purely azimuthal, i.e. $\psi = \eta = 0$, $\Gamma \neq 0$, and the vorticity in the bulk is initially normal to the interface, then if the surfactant system has a very small surface shear viscosity, the flow behaves as if the surface is clean, regardless of the elastic properties of the surfactant. This was dramatically demonstrated in recent experiments (Hirsa et al., 1995).

The surface tension, σ^* , and the surface shear and dilatational viscosities, μ^s and κ^s , depend on the thermodynamic state of the interface and thus are functions of the surface concentration of the surfactant, c^* . Most previous theoretical considerations have used a linear equation of state, i.e. $\sigma^* \propto c^*$, and have either set μ^s and κ^s to zero, or by linearizing about an equilibrium state have taken them to be constant coefficients. These linearizations are strictly only valid about an equilibrium concentration level. In problems where there is significant surface velocity, the concentration can be locally far from equilibrium and the nonlinearity of the equation of state and variations in μ^s and κ^s with surfactant concentration need to be taken into account.

Experiments (Gains, 1966; Poskanzer and Goodrich, 1975; Kim, 1996; Hirsa et al., 1997b) have measured the equation of state for a variety of surfactant/water systems (stearic acid, hemicyanine, and oleyl alcohol), and they can be modeled by an equation

$$\sigma^* - \sigma_i = -\frac{\delta}{\pi} \tan^{-1} \beta \left(\frac{c^* - c_i}{c_i} \right), \quad (2.6)$$

where the dimensional surfactant concentration, c^* , and surface tension, σ^* , are to be nondimensionalized by c_i and σ_i , the concentration and surface tension at the inflection point of the equation of state, respectively; δ is the saturation surface pressure, i.e. the range in surface tension between that of a clean air/water interface and that of the surfactant-saturated interface. It should be noted that the extrapolation of this model to large c^* , as suggested in Fig. 2, is dangerous as many surfactant systems, and in particular stearic acid/water and hemicyanine/water, may undergo molecular reorientation or phase changes for increasing c^* . We characterize a surfactant system by two parameters, a Marangoni number $M = -(c_i/\sigma_i)(\partial\sigma^*/\partial c^*)$ evaluated at $c^* = c_i$ and $\beta = M\pi\sigma_i/\delta$.

For the surface dilatational viscosity κ^s , there is no generally accepted measurement over a range of surfactant concentration (Edwards et al., 1991). For now, we will model both μ^s and κ^s with $\mu^s(c^*)$ and $\kappa^s(c^*) \rightarrow 0$ as $c^* \rightarrow 0$, and both $\mu^s(c^*)$ and $\kappa^s(c^*) \rightarrow \text{constant}$ as $c^* \rightarrow \infty$. A simple ad hoc function for the dimensionless surface viscosities $\lambda_\mu(c)$ and $\lambda_\kappa(c)$ will be used in this initial study:

$$\lambda_\mu = \Lambda_\mu \frac{c}{c+1}, \quad \text{and} \quad \lambda_\kappa = \Lambda_\kappa \frac{c}{c+1}, \quad (2.7)$$

where $\lambda_\kappa(c) \rightarrow \Lambda_\kappa$ and $\lambda_\mu(c) \rightarrow \Lambda_\mu$ as $c \rightarrow \infty$.

For insoluble surfactants on a nondeforming interface, the transport equation of c is given by

$$\frac{\partial c}{\partial t} + \nabla_s \cdot (c\mathbf{u}^s) = \frac{1}{\text{Pe}^s} \nabla_s^2 c, \quad (2.8)$$

where $\text{Pe}^s = \Omega R/D^s$ is the surface Peclet number and D^s is the coefficient of interfacial diffusivity, and \mathbf{u}^s is the dimensionless surface velocity, using ΩR as the velocity scale. Equation (2.8) is solved, along with the evolution equations for Γ and η in the interior, with $\partial c/\partial r = 0$ at $r = 0$ and 1, to give $c(r)$ at each time level, from which $\partial c/\partial r$ is obtained. The boundary conditions on c , together with $u = 0$ at $r = 0$ and 1, ensure that the insoluble surfactant is conserved on the enclosed domain $r \in [0, 1]$. The term $\partial\sigma/\partial r$ in (2.5) can be obtained from $\partial\sigma/\partial r = d\sigma/dc \partial c/\partial r$, where $d\sigma/dc$ is determined from the appropriate equation of state and $\partial c/\partial r$ from (2.8). The gradients $\partial\lambda_\mu/\partial r$ and $\partial\lambda_\kappa/\partial r$ in (2.4) and (2.5) are obtained in the same fashion using the model Eqs. (2.7).

3 Coupling of the Interface Dynamics to the Bulk Flow

The axisymmetric Navier-Stokes Eqs. (2.1) and (2.2) are solved using a second-order accurate in both time and space finite-difference scheme. Second-order central differences are used for all terms except the time derivatives. The advection-diffusion equation for c is also discretized in space using central differences in r and second-order one-sided differences in z at the interface. A two-stage second-order predictor-corrector scheme is used for temporal evolution; the scheme is essentially the same as that previously used in related problems (e.g., Lopez, 1990, 1995; Lopez and Weidman, 1996; Lopez and Shen, 1998), with the distinction being the implementation of the interfacial conditions.

The gas/liquid interface is treated as nondeforming, so that it is a flat stream-surface. The surface boundary condition on ψ is that ψ is constant and continuous with the flow on the axis. We can take $\psi = 0$ on the surface. That leaves η and Γ , and their boundary conditions are given by the solutions to (2.4) and (2.5). In the explicit scheme used, η and Γ on the interior grid points are updated to the new time-level first. Then the left-hand side of (2.4) can be written as a second order one-sided difference approximation to the normal derivative. This approximation is in terms of the just updated values of Γ one and two grid points in from the surface and the yet unknown value of Γ on the surface. Equation (2.4) then becomes a second-order ordinary differential equation for Γ on the surface, with $\Gamma = 0$ at $r = 0$ and 1. Using second-order central differences, this results in a tridiagonal system and is readily solved by standard techniques (e.g., LAPACK routines).

The boundary condition on η is a little more involved. The viscous terms couple the surface condition with the recently updated interior flow (as in the case for Γ above). Here, we first compute $\partial\psi/\partial z$ on the surface using second-order one-sided differences of the solution to $\nabla_s^2 \psi = -r\eta$ with the updated η on the right-hand side. Then, $\partial(\partial\psi/\partial z)/\partial r$ and $\partial^2(\partial\psi/\partial z)/\partial r^2$ are formed using center-differences and one-sided differences at $r = 0$ and 1. In this way, the viscous contribution to

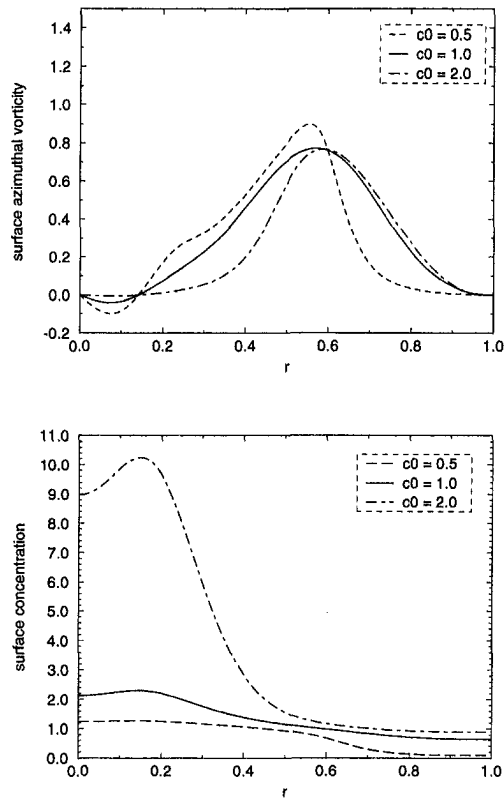


Fig. 3 Influence of different initial uniform concentrations on (a) the elastic production of surface azimuthal vorticity and (b) the redistribution of surfactant for a surfactant system with the hemicyanine/water equation of state, neglecting surface viscosity effects, at steady state for $Re = 2126$, $H/R = 2.5$

η on the surface is calculated. The elastic contribution (both the viscous and the elastic contributions are imposed simultaneously) requires information concerning the surface tension gradients $\partial\sigma/\partial r$.

4 Results

In our model problem, the fluid in the open cylinder is initially at rest. Before any fluid motion, the surfactant is uniformly distributed on the free surface. The initial concentration of surfactant, c_0 , is low enough to be considered as a monomolecular layer (monolayer). Note that in general $c_0 \neq 1$. At $t = 0$, the bottom endwall is impulsively set to rotate at constant angular speed Ω . An Ekman boundary layer develops on the rotating disk with thickness of $O(Re^{-1/2})$. This rotating boundary layer sends fluid radially outwards in a spiraling motion while drawing fluid into it from above. A sidewall boundary layer is also established. In time, fluid with angular momentum reaches the vicinity of the surface covered by the surfactant monolayer, where it is turned and advected towards the center. This flow results in a nonuniform distribution of the surfactant, with an accumulation of the surfactant near the center.

4.1 Nonlinear Equation of State Effects and Elastic Interfaces. Herein, we use three different insoluble surfactant groups, stearic acid, hemicyanine, and oleyl alcohol with water as the bulk fluid. Molecules within a monolayer at a gas/liquid interface can exist in different states, analogous to three-dimensional liquid, solid, or gas states (Adamson, 1982). Stearic acid is a solid-like surfactant (Gains, 1966) with relatively large viscosities, hemicyanine is known (Hirsa et al., 1995) to change from liquid-like to solid-like behavior at large concentration, and oleyl alcohol is a liquid-like surfactant with low viscosities but strong elastic behavior. For stearic acid/water $M = 0.43$

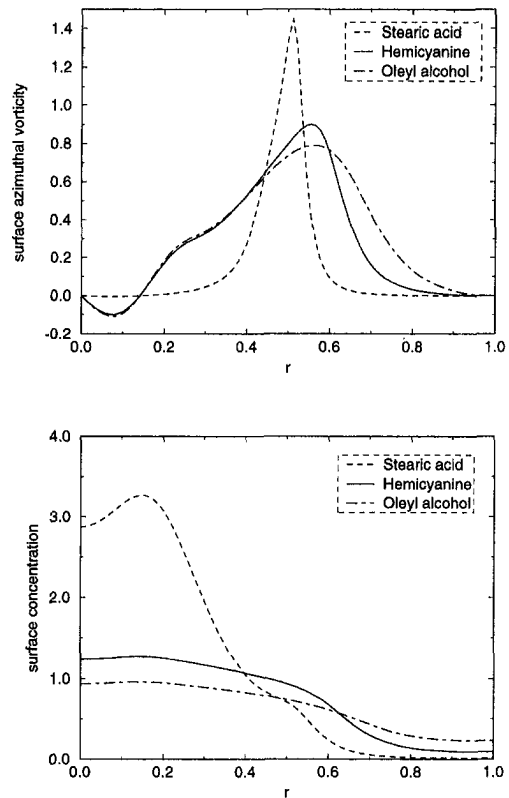


Fig. 4 Influence of different equations of state on (a) the elastic production of surface azimuthal vorticity and (b) redistribution of surfactant ($c_0 = 0.5$), at steady state for $Re = 2126$, $H/R = 2.5$

and $\beta = 5.62$, for hemicyanine/water $M = 0.51$ and $\beta = 3.90$, and for oleyl alcohol/water $M = 0.72$ and $\beta = 3.27$.

We first investigate the elastic effects of surfactants caused solely by surface tension gradients. In general, the elasticity of the surface depends strongly on both the composition of the surfactant, as well as the surfactant concentration. The influence of the initial surfactant concentration on a system with an equation of state corresponding to hemicyanine is shown in Fig. 3 (note that here we only consider surface tension gradient effects and are setting the interface to be inviscid, i.e., elastic; Section 4.2 treats the viscoelastic case incorporating the surface viscosities). The presence of surfactants generally lowers the local interfacial tension, and the variation in surfactant concentration gives rise to surface tension gradients and establishes a closed-loop interaction among the hydrodynamic motion, surfactant

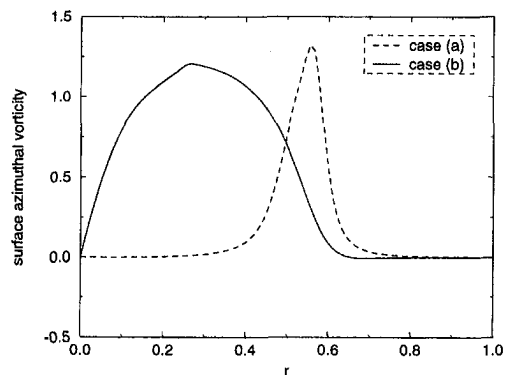


Fig. 5 Influence of surface shear and dilatational viscosities on the production of surface azimuthal vorticity for $Re = 2126$, $H/R = 2.5$, $M = 0.43$, $\beta = 5.62$, $Pe^s = 500$, and $c_0 = 0.5$: (a) elastic interface, $\Lambda_\mu = \Lambda_x = 0.0$; (b) viscoelastic interface $\Lambda_\mu = 1.0$ and $\Lambda_x = 5.0$

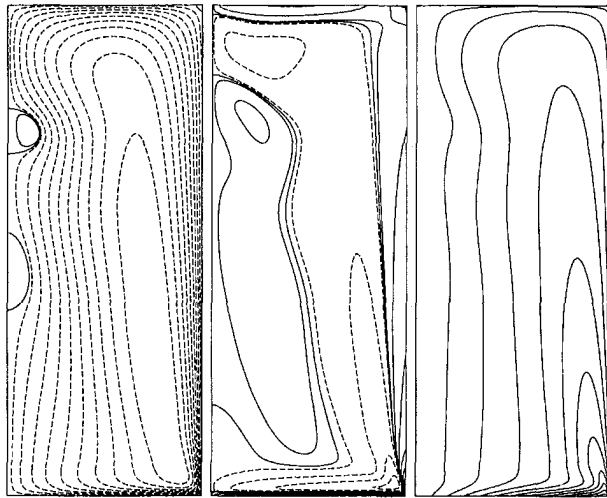


Fig. 6(a) Contours at steady state of ψ , η , and Γ for $Re = 2126$ and $H/R = 2.5$ for a no-slip stationary top

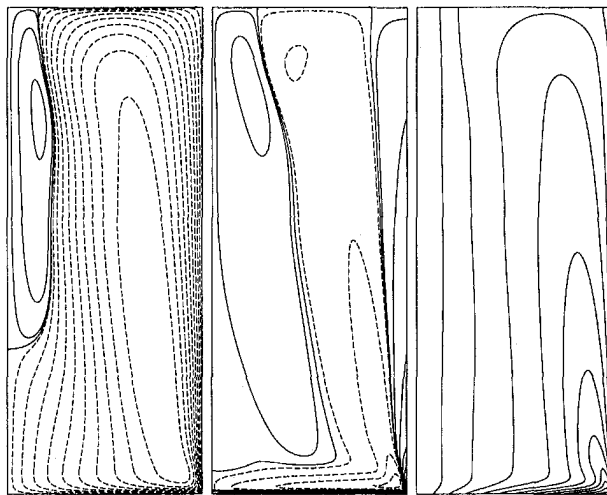


Fig. 6(b) Contours at steady state of ψ , η , and Γ for $Re = 2126$ and $H/R = 2.5$ for a clean stress-free top surface

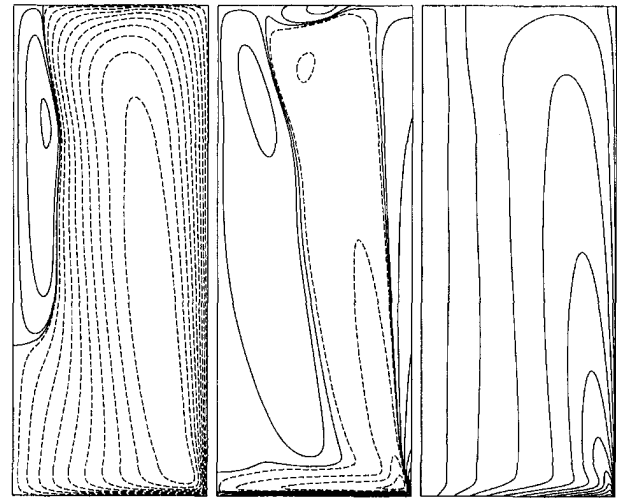


Fig. 6(c) Contours at steady state of ψ , η , and Γ for $Re = 2126$ and $H/R = 2.5$ for surfactant contaminated top with $M = 0.43$, $\beta = 5.62$, $\Lambda_x = 0$, and $\Lambda_\mu = 0$ (elastic)

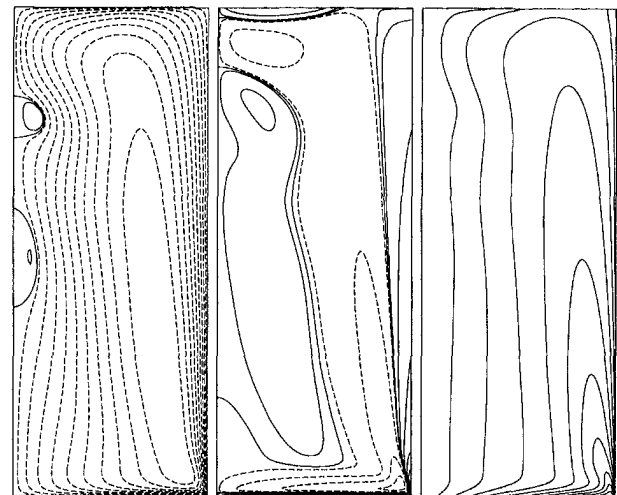


Fig. 6(d) Contours at steady state of ψ , η , and Γ for $Re = 2126$ and $H/R = 2.5$ for surfactant contaminated top with $M = 0.43$, $\beta = 5.62$, $\Lambda_x = 5$, and $\Lambda_\mu = 1$ (viscoelastic)

concentration, and surface tension. This is referred to as a Marangoni effect. We observe in Fig. 3(a) that an azimuthal component of vorticity is produced on the surface. At larger initial concentration ($c_0 = 2.0$) the surface tension gradient tends to zero (see Fig. 2) which diminishes the elastic production of surface azimuthal vorticity.

Of the three surfactant systems considered, oleyl alcohol/water has the strongest elastic behavior and stearic acid the weakest (see Fig. 2). For $Re = 2126$, $H/R = 2.5$ flows with all three systems, as well as flows with a clean interface and with a stationary no-slip top, reach steady state within one or two hundred rotations of the bottom endwall. All the cases shown in this paper were computed using a uniform grid with 91 radial and 226 axial nodes and a time increment of 10^{-2} . These spatial and temporal resolutions were previously found (e.g., Lopez, 1990, 1995) for the rigid top and stress-free surface cases to give grid independent results. Tests with the elastic and viscoelastic surfaces also indicate that these resolutions are adequate. The steady-state distribution of the surface azimuthal vorticity for the three surfactant systems (due only to elastic interfacial processes) is given in Fig. 4(a), along with the corresponding distribution of surface concentration of the surfactants in Fig. 4(b). The initial uniform concentration was $c_0 = 0.5$. In considering elastic interfaces, the presence of surfactants has no direct influence on Γ at the interface and η is only affected through the surface tension gradients. The bulk motions

near the interface redistribute the surfactant. The flow near the interface consists primarily of a swirling flow spiraling radially inwards. For a clean interface, conservation of angular momentum (see discussions in Spohn et al., 1993 and Lopez, 1995) leads to a recirculation cell attached to the interface near the axis, where the radial flow on the interface is outwards. With elastic interfaces, similar behavior is found. The redistribution of surfactant by advection is resisted by diffusive processes (all cases in Fig. 4 had a surface Peclet number of 500) and the elastic force due to surface tension gradients. We see that the least elastic system (stearic acid) suffers the most redistribution, with the outer part of the interface ($r > 0.8$) being virtually clean and there is a corresponding large build up of surfactant for $r < 0.1$ where the level is well beyond saturation, i.e. surface tension gradients vanish. So, even though there are strong variations in concentration throughout $0 \leq r \leq 1$ for stearic acid, the elastic production of surface azimuthal vorticity is restricted to $0.35 < r < 0.65$ due to the nonlinearity of the equation of state.

For the more elastic cases, the redistribution of surfactant is far less and is everywhere below saturation levels. The outer parts of the interface are still cleaned somewhat, but the production of surface azimuthal vorticity is more wide spread, although at a lower peak intensity, than with stearic acid. The recircula-

tion near the axis leads to a reversal in the concentration gradient there and the production of negative surface azimuthal vorticity. The same would have occurred with stearic acid if the concentration there had not been at saturation levels. This suggests, that in these type of flows, a build up of a boundary layer type flow near the axis would be more pronounced for lower initial concentration levels c_0 .

4.2 Viscoelastic Interfaces. The discussion so far has concerned elastic interfaces, where we have artificially set the surface shear and dilatational viscosities to zero. Now, we include their dynamic effects via the model Eq. (2.7). In this study, we use this ad hoc model as the available rheological information needed is lacking. Incorporating surface shear and dilatational viscosities according to (2.7) with $\Lambda_\mu = 1.0$ and $\Lambda_\kappa = 5.0$, we first investigate how this influences the production of surface azimuthal vorticity for a surfactant system with the equation of state corresponding to stearic acid.

The inclusion of surface viscosities results not only in a quantitative change, but also a qualitative change in the characteristics of the flow. The production of surface azimuthal vorticity is shifted and extended over a much broader central area (see Fig. 5). A number of factors are at play here, all interacting nonlinearly. Whereas for the elastic case the only contribution to η on the surface comes from surface tension gradients, in the viscoelastic situation the right-hand side of (2.5) includes a viscous contribution due to the surface flow and the bulk flow near the surface. Also, the right-hand side of (2.4) is no longer zero, and this leads to vortex line bending at the surface ($\partial\Gamma/\partial z \neq 0$) which contributes to the production of η via the $-1/r^3 \partial\Gamma^2/\partial z$ term in (2.2). Note that this vortex line bending at the interface, i.e. vortex lines not meeting the interface normally, is only possible for viscous interfaces, regardless of the concentration level. These surface viscosity-influenced productions of surface vorticity alter the surface flow and result in a different distribution of surfactant concentration, which in turn alters the distribution of surface tension gradients. All of these processes are coupled nonlinearly; they affect not only the surface flow and the bulk flow immediately adjacent to the interface, but also produce large scale global changes in the bulk flow.

In order to gain an impression of the global effects of a viscoelastic interface, we compare the steady state flow when the top is stationary no-slip, a clean free surface, surfactant contaminated with $M = 0.43$, $\beta = 5.62$, $Pe^s = 500$, $\Lambda_\kappa = 5.0$, and $\Lambda_\mu = 1.0$ (viscoelastic), and $\Lambda_\kappa = \Lambda_\mu = 0.0$ (elastic). The corresponding contours of ψ , η , and Γ are presented in Fig. 6.

On the no-slip stationary endwall the fluid separates at $r = 0$ and a central vortex is formed whose core size depends on the thickness of the boundary layer from which it emerged (Fig. 6(a)). For a clean stress-free top surface there is a large recirculation zone on the axis attached to the free surface, producing a reversed (directed radially outwards) surface flow near the axis (Fig. 6(b)). The boundary layers caused by the accumulation of surfactant materials are shown in Figs. 6(c) and 6(d). When the surface viscosities are set to zero, the elastic production of surface azimuthal vorticity is localized (Fig. 6(c)). Comparing the elastic case with the clean surface case, we find that the presence of inviscid surfactants has virtually no effect on Γ ; whereas, the viscous contributions are seen to cause substantial vortex line bending, particularly for $r < 0.65$ where the concentration of surfactant is largest in the viscoelastic case (Fig. 6(d)). Note that if the flow were planar two-dimensional, there would be no flow component corresponding to Γ , and hence the surface vorticity production associated with vortex line tilting, i.e., $\partial\Gamma/\partial z \neq 0$ at the interface, which is only active for viscous surfactants, would not exist. So, if the flow is planar two-dimensional, this mechanism of surface vorticity production, whose predominance depends on the viscous nature of the interface, is not present regardless of how viscous the interface may be. For planar two-dimensional flows, the

vorticity has only one nonzero component and it corresponds essentially to η in the present axisymmetric flow, so surface viscosity effects will also be present in planar two-dimensional flows via the corresponding viscous terms in (2.5).

In comparing all four cases shown in Fig. 6, it is very striking that although the elastic production of surface vorticity is active with inviscid interfaces, it only produces a very localized effect and the resultant bulk flow is a small perturbation away from that when the surface is stress-free. However, inclusion of the surface viscosity terms causes a dramatic global change in the flow. The surface layer that results is as intense as the boundary layer due to the stationary no-slip top. The resultant bulk flow is very similar to that of the no-slip case, but the vortex breakdown recirculation cells on the axis are more intense for the viscoelastic case. In fact, although the same Re is used in both cases, the viscoelastic surfactant bulk flow has characteristics of a bulk flow with a no-slip top at a higher Re .

5 Conclusions

The viscoelastic effects due to the presence of insoluble surfactants on the surface of a swirling vortex flow have been investigated numerically. The hydrodynamic coupling between the bulk swirling flow and the surfactant-covered surface flow is provided via the tangential stress balance at the interface, and this balance is dependent upon the surface concentration of surfactant, which in turn is altered by the interaction of bulk and surface flows. The viscoelastic properties of surfactants are functions of the surfactant concentration, for which we are presently using ad hoc models until they are determined experimentally. We investigate not only the elastic influence caused solely by surface tension gradients of different surfactant groups and surfactant concentration, but also surface viscosity effects caused by both surface dilatational and shear viscosities. Comparisons among stress-free clean top surfaces, no-slip tops, and contaminated surface flows provide a first look at the dynamics of flows where the inner product of the surface velocity and surface vorticity is not identically zero and the surface viscosities are treated as functions dependent upon the surfactant concentration. It is clear from this preliminary investigation that the viscous properties of a surfactant influenced interface can have a dramatic quantitative and qualitative impact on both the interfacial and the bulk flows, not only local to the interface, but also globally. This is so even at relatively low concentration levels of surfactant. In a future study, we will include soluble surfactants, deforming free surfaces, as well as incorporating empirically determined viscoelastic properties of the surfactants into our numerical simulation.

Acknowledgments

We would like to thank Prof. Amir Hirsra for the many discussions and sharing his data. This work was partially funded by NSF grants DMS-9512483 and CTS-9896259 and some of the computations were performed at NCSA.

References

- Adamson, A. W., 1982, *Physical Chemistry of Surfaces*, Wiley-Interscience Publication.
- Ananthakrishnan, P., and Yeung, R. W., 1994, "Nonlinear Interaction of a Vortex Pair with Clean and Surfactant-Covered Free Surfaces," *Wave Motion*, Vol. 19, pp. 343–365.
- Asher, W. E., and Pankow, J. F., 1991, "Prediction of Gas/Water Transport Coefficients by a Surface Renewal Model," *Environmental Science and Technology*, Vol. 25, pp. 1294–1300.
- Boussinesq, J., 1913, "Sur l'existence d'une viscosité superficielle, dans la mince couche de transition séparant un liquide d'un autre fluide contigu," *Comptes Rendus Hebdomadaires des Séances de l'Académie des Sciences*, Vol. 156, pp. 983–989.
- Edwards, D. A., Brenner, H., and Wasan, D. T., 1991, *Interfacial Transport Processes and Rheology*, Butterworth-Heinemann, Washington DC.
- Foda, M., and Cox, R. G., 1980, "The Spreading of Thin Liquid Films on a Water-Air Interface," *Journal of Fluid Mechanics*, Vol. 101, pp. 33–51.

- Gains, G. L., 1966, *Insoluble Monolayers at Liquid-Gas Interfaces*, Interscience Publishers.
- Grotberg, J. B., 1994, "Pulmonary Flow and Transport Phenomena," *Annual Reviews of Fluid Mechanics*, Vol. 26, pp. 529–571.
- Hirsa, A., Harper, J. E., and Kim, S., 1995, "Columnar Vortex Generation and Interaction with a Clean or Contaminated Free Surface," *Physics of Fluids*, Vol. 7, pp. 2532–2534.
- Hirsa, A., Korenowski, G. M., Logory, L. M., and Judd, C. D., 1997a, "Velocity Field and Surfactant Concentration Measurement Techniques for Free-Surface Flows," *Experiments in Fluids*, Vol. 22, pp. 239–248.
- Hirsa, A., Korenowski, G. M., Logory, L. M., and Judd, C. J., 1997b, "Determination of Surface Viscosities by Surfactant Concentration and Velocity Field Measurements for an Insoluble Monolayer," *Langmuir*, Vol. 13, pp. 3813–3822.
- Hirsa, A., Korenowski, G. M., Logory, L. M., Judd, C. J., and Kim, S., 1995, "Surfactant Effects on Vortex Flows at a Free Surface and the Relation to Interfacial Gas Transfer," *Air-Water Gas Transfer*, B. Jahne and E. C. Monahan, eds., AEON Verlag Publishing, Heidelberg, Germany, pp. 649–663.
- Hunt, J. C. R., 1984, "Turbulent Structure and Turbulent Diffusion Near Gas-Liquid Interfaces," *Gas Transfer at Water Surfaces*, W. Brutsaert and G. H. Jurka, eds., D. Reidel, Boston pp. 67–82.
- Kim, S., 1996, "An Experimental Investigation of a Columnar Vortex Terminating Normal to a Gas/Liquid or a Solid/Liquid Interface," Ph.D. thesis, Aeronautical Eng., Rensselaer Polytechnic Institute.
- Lopez, J. M., 1990, "Axisymmetric Vortex Breakdown. Part I. Confined Swirling Flow," *Journal of Fluid Mechanics*, Vol. 221, pp. 533–552.
- Lopez, J. M., 1995, "Unsteady Swirling Flow in an Enclosed Cylinder with Reflectional Symmetry," *Physics of Fluids*, Vol. 7, pp. 2700–2714.
- Lopez, J. M., and Shen, J., 1998, "An Efficient Spectral-Projection Method for the Navier-Stokes Equations in Cylindrical Geometries," *Journal of Computational Physics*, Vol. 139, pp. 308–326.
- Lopez, J. M., and Weidman, P. D., 1996, "Stability of Stationary Endwall Boundary Layers During Spin-Down," *Journal of Fluid Mechanics*, Vol. 326, pp. 373–398.
- Maru, H. C., and Wasan, D. T., 1979, "Dilational Viscoelastic Properties of Fluid Interfaces—II," *Chemical Engineering Science*, Vol. 34, pp. 1295–1307.
- Poskanzer, A., and Goodrich, F. C., 1975, "A New Surface Viscometer of High Sensitivity: II. Experiments with Stearic Acid Monolayers," *Journal of Colloid and Interface Science*, Vol. 52, pp. 213–221.
- Scriven, L. E., 1960, "Dynamics of a Fluid Interface," *Chemical Engineering Science*, Vol. 12, pp. 98–108.
- Slattery, J. C., 1990, *Interfacial Transport Phenomena*, Springer-Verlag, NY.
- Spohn, A., Mory, M., and Hopfinger, E. J., 1993, "Observations of Vortex Breakdown in an Open Cylindrical Container with a Rotating Bottom," *Experiments in Fluids*, Vol. 14, pp. 70–77.
- Sternling, C. V., and Scriven, L. E., 1959, "Interfacial Turbulence: Hydrodynamic Instability and the Marangoni Effect," *American Institute of Chemical Engineers Journal*, Vol. 5, pp. 514–523.
- Tryggvason, G., Abdollahi-Alibeik, J., Willmarth, W. W., and Hirsa, A., 1992, "Collision of a Vortex Pair with a Contaminated Free Surface," *Physics of Fluids A*, Vol. 4, pp. 1215–1229.
- Tsai, W.-T., and Yue, K. P., 1995, "Effects of Soluble and Insoluble Surfactant on Laminar Interactions of Vortical Flows with a Free Surface," *Journal of Fluid Mechanics*, Vol. 289, pp. 315–349.
- Wang, H. T., and Leighton, R. I., 1990, "Direct Calculation of the Interaction Between Subsurface Vortices and Surface Contaminants," *Proceedings of the 9th OMAE Conference*, Houston, TX, Feb., ASME, NY, Vol. I, Part A.